

Cell-by-cell scanning of whole mitochondrial genomes in aged human heart reveals a significant fraction of myocytes with clonally expanded deletions

Konstantin Khrapko^{1,2,*}, Natalya Bodyak^{1,2}, William G. Thilly², Nathalie J. van Orsouw³, Xiaomin Zhang¹, Hilary A. Collier⁴, Thomas T. Perls¹, Melissa Upton⁵, Jan Vijg³ and Jeanne Y. Wei¹

¹Gerontology Division, Beth Israel Deaconess Medical Center and Harvard Medical School, Boston, MA 02115, USA, ²Center for Environmental Health Sciences, Massachusetts Institute of Technology, Cambridge, MA 02139, USA, ³University of Texas Health Science Center, San Antonio, TX 78229, USA, ⁴Fred Hutchinson Cancer Research Center, Seattle, WA 98109, USA and ⁵Department of Pathology, Beth Israel Deaconess Medical Center and Harvard Medical School, Boston, MA 02115, USA

Received October 16, 1998; Revised and Accepted April 15, 1999

ABSTRACT

Quantitative information on the cell-to-cell distribution of all possible mitochondrial DNA (mtDNA) mutations in young and aged tissues is needed to assess the relevance of these mutations to the aging process. In the present study, we used PCR amplification of full-length mitochondrial genomes from single cells to scan human cardiomyocytes for all possible large deletions in mtDNA. Analysis of more than 350 individual cells that were derived from three middle-aged and four centenarian donors demonstrates that while most of the cells contain no deletions, in certain cardiomyocytes a significant portion of the mtDNA molecules carried one particular deletion. Different affected cells contained different deletions. Although similar numbers of cells were screened for each donor, these deletion-rich cells were found only in the hearts of old donors, where they occurred at a frequency of up to one in seven cells. These initial observations demonstrate the efficiency of the method and indicate that mitochondrial mutations have the potential to play an important role in human myocardial aging.

INTRODUCTION

About 10 years ago it was proposed that aging is caused by life-long accumulation of somatic mitochondrial DNA (mtDNA) mutations (1), which compromises cellular energy metabolism and/or increases intracellular oxidative stress (2). Ultimately, this could result in the development of the multiple degenerative changes in tissues that become manifest in old age. It has been shown that mtDNA deletions and, with less certainty, mtDNA point mutations, increase with advancing age (recently reviewed in 3,4). These data are consistent with the mitochondrial theory

of aging but do not exclude the possibility that accumulation of mtDNA mutations accompanies, but does not cause aging.

To discriminate between the two possibilities, it would be important to explore whether these mutations are physiologically relevant and whether the expected damage caused by these mutations is sufficient to account for age-related changes in tissues. A natural way to address this question is first to study age-related changes in tissues and then relate them to somatic mtDNA mutations. This approach, however, is complicated by the intricacy of the aging phenotype. Instead, we propose a 'reversed' approach: to perform detailed measurements of mtDNA mutations and to infer, based on this information, whether mtDNA mutations are likely to play a major role in aging.

Since there are multiple copies of mitochondrial genomes per cell, a mtDNA mutation may become physiologically relevant for a given cell only if the mutant fraction in that particular cell exceeds a certain threshold (5). Therefore, we reasoned that to assess their relevance, somatic mtDNA mutants must be measured directly in individual cells rather than in homogenized tissue. The cells with substantial fractions of mtDNA mutations (if found) are likely to be adversely affected by these mutations. Moreover, measuring one or a few particular mutations out of many possible varieties is not sufficient. The majority of cells with defects that result from other untested types of mtDNA mutations would thereby escape analysis. In order to obtain a representative estimate of possible tissue damage caused by mtDNA mutations, individual cells must be scanned for all (or a significant proportion of all) possible mtDNA mutations.

Mitochondrial mutations in single cells have been studied in tissues affected by mitochondrial disease by *in situ* hybridization (e.g. 6–8) as well as by allele-specific PCR amplification and restriction digestion analysis (e.g. 9). These methods require prior knowledge of the type of the mutation. Similar studies are more difficult to perform in healthy aged tissues, because, in contrast

*To whom correspondence should be addressed at: Harvard Institutes of Medicine, Room 921, 77 Avenue Louis Pasteur, Boston, MA 02115, USA.
Tel: +1 617 6670973; Fax: +1 617 667 0980; Email: khrapko@wccf.mit.edu

to diseased tissue, in this case it is not known a priori what mutations should be sought. As a result, there has been only a limited number of such studies, which are based either on numerical analysis of the results of allele-specific PCR from small numbers of cells (10,11), or on *in situ* hybridization (12). An important conclusion from these studies is that mitochondrial mutations are apparently segregated within a tissue, i.e. while some cells contain substantial amounts of mutants, others lack detectable mutants.

Most studies of somatic mtDNA mutations, including those cited above, have focused on a few particular mutations out of the many possible ones. Recently, several PCR-based procedures were developed for the detection of all possible mtDNA deletions in tissue homogenates. These procedures are based either on long-distance PCR (13–15) or on PCR amplification with multiple primers (16). These studies yielded conflicting results regarding the total load of deletions (see Discussion) and were not able to address the issue of cell-to-cell distribution of these mutants.

To overcome the limitations of existing methods, we developed an approach to scan individual cells for all possible mtDNA deletions by amplifying full-length mitochondrial genomes from individual cells. The novelty of this approach is that it was able to combine single cell analysis with measurement of all possible mtDNA deletions, which was not possible before. Herein we report the results of such scanning of myocytes from human hearts of different ages. The implications of our findings to the mitochondrial theory of aging and the prospects of extending this approach to scanning of individual cells for all possible mtDNA mutations including point mutations are discussed.

MATERIALS AND METHODS

Isolation of individual cardiomyocytes

Human autopsy heart samples (left ventricle, free wall) were collected within several hours after death, quickly frozen in liquid nitrogen, and stored at -80°C . To make a cell suspension, frozen tissue was sliced with a razor blade to make slices ~ 0.1 mm thick, ~ 10 mg each. The slices were transferred into 15 ml Krebs–Henseleit buffer (Sigma), supplemented with 0.1 mg/ml collagenase (Worthington), 10 mM EDTA pH 8 and 0.03% Evans Blue dye (Sigma) in a Petri dish and put on an orbital shaker for 1 h at 100 r.p.m. at room temperature. Individual cardiomyocytes were isolated using a modification of the method, which was described for skeletal muscle (9). Individual cells were picked under inverted microscope by a hand-held siliconized glass capillary (~ 50 μm I.D.), pulled from a Pasteur pipette, and transferred to individual thin-wall 0.5-ml PCR tubes. The capillary was connected to a mouthpiece and finely controlled mouth pressure was used to draw and expel cells in and out of the capillary pipette. Each processed cell was photographed for future reference (examples are shown in Fig. 1). The procedure is straightforward; it takes <5 min to process a cell.

DNA isolation and amplification

To liberate the DNA, each cell in a 0.5 ml tube was covered with 1 μl of 10 mM EDTA pH 8, 0.5% SDS and 2 mg/ml proteinase K, and incubated for 30 min at 37°C . The samples were then diluted 10-fold with water by gentle pipetting.

The DNA from individual cells was subjected to long-distance nested PCR using TaKaRa LA PCR system (Panvera, Madison,

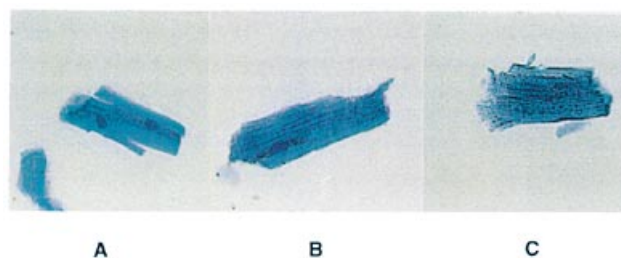


Figure 1. Individual human cardiomyocytes. Cardiomyocytes were isolated as described in the text. (A–C) represent the typical appearance of the cells. The cell in (C) contains $\sim 25\%$ of a deleted mtDNA species 9.1 kb long.

WI). The outer pair of primers d(CACCCTATGTCGCAG-TATCTGTCTTTGATTCCTGCCTCATC) and d(AGGGGA-ACGTGTGGGCTATTTAGGCTTTATGACCCTGAA) was used to amplify the fragment from bp 110 to bp 16 550 of the human mitochondrial genome. The inner nested pair of primers d(TCGCACCTACGTTCAATATTACAGGCGAACATAC) and d(TAGGAACCAGATGTCGGATACAGTTCACTTTAGC) was used to amplify the fragment from bp 161 to bp 16 510 of the human mitochondrial genome (GenBank accession no. V00662). Negative PCR controls were performed on a regular basis and were always negative.

To inactivate proteinase K, 1 μl of the DNA solution (that is, 1/10 of DNA isolated from a single cell) was added to 5 μl of $1\times$ TaKaRa LA buffer and incubated for 1 min at 95°C . The sample was supplemented with the remaining TaKaRa LA PCR components (total volume of 20 μl , with the outer pair of primers) and subjected to 25 cycles of long distance PCR according to the manufacturer's protocol (cycle: 20 s at 95°C , 10 min at 68°C). One μl of PCR product was added to 20 μl of fresh reaction components (with inner pair of nested primers) and subjected to additional 20 cycles of PCR.

Detection and measurement of mtDNA deletions

PCR products were separated by gel electrophoresis in 0.7% agarose and visualized by standard ethidium bromide staining. The gel images were captured, digitized and quantified using a CCD-based image analysis system. Multiple exposures were used to ensure that the signal was within the linear range of the measuring system. A cell was considered a candidate carrier of a deletion if a prominent PCR product of a lower molecular weight was observed in addition to the full-length mtDNA. A separate aliquot of DNA from these cells was subjected to a duplicate PCR. The deletion was considered confirmed if the duplicate PCR revealed the same deleted product as the first one.

The resolution of our electrophoresis system was sufficient to detect differences in length of $\sim 3\%$, so we should have been able to detect deletions of as little as 500 bp. Potentially, we should have been able to detect partial duplications in mtDNA, which do not include PCR primer region around the origin of replication of mtDNA if such duplications were present in the cells we analyzed. However, the sensitivity of detection of such partial duplications would have been much lower than that of deletions, because low intensity 'duplication' bands above the wild-type PCR product would have been lost in the 'smear' emanating upwards from the intense wild-type band (Fig. 2).

The ratio of the shorter (deleted) to the full-length (wild-type) PCR product does not necessarily reflect the original ratio of wild-type to deleted mtDNA in the cell, since shorter fragments may be amplified with a higher efficiency which would result in their over-representation in the final PCR product. To infer the original fraction of a deletion in a cell, the ratio of the deleted to the full-length product was corrected for the observed differences in amplification efficiencies of the two species. The relative amplification efficiencies were determined based on reconstruction experiments as described in the Results.

Determination of deletion breakpoints

We have devised an economical and efficient approach to determine the breakpoints of mtDNA deletions. A detailed description of the approach will be presented elsewhere (N.D.Bodyak, J.Y.Wei and K.Khrapko, manuscript in preparation). Briefly, deleted mtDNA was digested in two separate reactions either by restriction endonuclease *Bst*NI or by a combination of *Ava*I, *Dra*I and *Bcl*II. The corresponding restriction sites in the wild-type mtDNA occur at least every 1000 bp and yet produce a pattern of restriction fragments which can be clearly separated from each other and unambiguously identified in 2% agarose gel. The set of restriction endonucleases which meet the above criteria was selected with the help of *tag2*, an excellent software product available free through a web site (17). The absence of certain restriction fragments from the pattern of digestion of a particular deleted mtDNA allowed us to map the deletion breakpoint to within 1000 bp. The appropriate PCR primers flanking the expected breakpoint were then selected and sequencing of the resulting PCR fragment in both directions yielded the exact sequence of the breakpoint.

RESULTS

Methodology: isolation of DNA from individual cells and long-distance PCR

To scan whole mitochondrial genomes of individual cells for mtDNA deletions we developed a new procedure that enabled us to perform long-distance single cell PCR. Human heart tissue was dissociated into single cells by collagenase treatment and cardiomyocytes were collected individually. To isolate DNA for amplification we used a miniature (1 μ l total volume) SDS/proteinase K digestion. We reasoned that the DNA impurities from a single cell should be insignificant and should not affect PCR efficiency. We therefore eliminated any further purification steps which could damage the high molecular weight PCR template. Of concern were proteinase K and SDS. Proteinase K was inactivated by pre-heating the sample prior to the addition of polymerase. SDS at the concentrations used in the procedure did not affect PCR efficiency. We also tried to use other procedures, such as alkaline lysis, commonly used for DNA liberation from single cells (9,18), as well as boiling of the cells in water or buffer. Neither of the two procedures worked in our hands for the preparation of long-distance PCR template, although we have successfully used them for short fragment PCR before.

This simple micro SDS/proteinase K procedure proved very efficient for preserving the integrity of long DNA fragments. The yield of undamaged mtDNA molecules was very high. We obtained on the order of 1000 amplifiable full-length mtDNA molecules per isolated cell, which was demonstrated by the fact

that as little as 1/100 of a single cell DNA preparation still produced reproducible PCR signal. The fact that this method preserves a large number of undamaged mtDNA copies per cell is very important for our ability to quantify mtDNA deletions. First, the probability that a deleted DNA molecule will be damaged during DNA isolation is lower than that for a full-length mtDNA. Our ability to preserve a large number of undamaged mtDNA copies therefore reduces the likelihood that we would overestimate the proportion of deletions due to such a bias. Second, PCR has a tendency to generate aberrant products of shorter length (see below). In cases where full-length mtDNA copies are scarce or absent, these aberrant products may prevail, creating an illusion of a high fraction of deleted mtDNA. Finally, the high yield of undamaged copies per cell allows us to perform multiple PCR amplifications from the same single cell DNA preparation, which enables us to eliminate the possibility that the deletions we report are PCR artifacts (see below).

DNA from each cardiomyocyte was subjected to nested long-distance PCR, capable of amplifying almost the full-length mitochondrial genome. The use of nested primers helped to eliminate low molecular weight products, presumably primer dimers and misprimed PCR fragments, which otherwise accumulated in significant amounts after approximately 30 cycles of PCR. Thus, we were able to clearly visualize PCR products by simple ethidium bromide staining without resorting to more sensitive but more laborious techniques. Finally, the use of nested PCR guaranteed that PCR products were of mitochondrial origin. Amplification of wild-type mtDNA resulted in a PCR fragment ~16.4 kb long, while deleted mitochondrial genomes produced shorter PCR fragments, which were resolved by gel electrophoresis. This procedure is able to detect almost all possible large mtDNA deletions with the exception of those that cannot be amplified because one of the primer sequences is affected by the deletion. We expect that these undetectable deletions are of limited importance because primer sequences are positioned very close to the origin of replication of mtDNA.

Cell-by-cell distribution of mitochondrial genomes with deletions

Analysis of PCR samples obtained from a large number of individual cells showed that the majority of samples contained only one major PCR product corresponding to the full-length mtDNA product (Fig. 2, lane 1). However, for a few cells (14 cells out of more than 350 cells analyzed, or 4%) we observed an additional intense band (one type per cell) corresponding to a PCR product of a shorter length representing mtDNA with a deletion. (Seven examples are given in Fig. 2, lanes 5–11.)

Note that in fact, lane 1 does contain additional low intensity bands. These background bands are seen more clearly in lane 2, where the same sample as in lane 1 was overloaded to reveal the low intensity background. These bands appear at similar relative intensities in all our PCR reactions, even when PCR is performed on just a few initial mtDNA molecules. This means that these bands represent deletions that are continuously generated by *Taq* polymerase during PCR (deletional 'hotspots'). Alternatively, these deletions could have been caused by mispriming during the initial PCR cycles. We ruled out such a possibility by demonstrating that these deleted mtDNA species could be amplified by a second internal set of nested primers (data not shown).

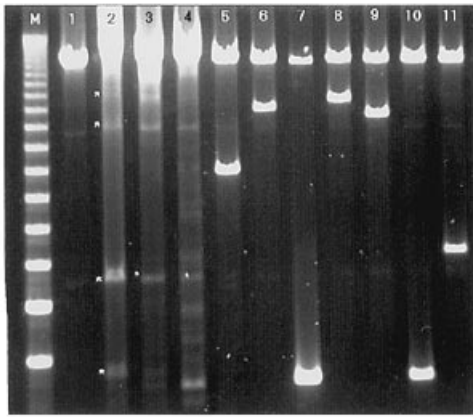


Figure 2. PCR of the whole mtDNA genome from individual cardiomyocytes. Lane 1, a typical PCR from a cell that does not contain deleted mtDNA. Lane 2, 'background bands' presumably generated by PCR (marked by asterisks); the same PCR reaction as in lane 1 is overloaded to reveal the low intensity bands. Lanes 3 and 4, PCR from DNA isolated from homogenized heart tissue of a 31 and a 101 year-old donor, respectively. Overloaded to visualize low intensity bands. Lanes 5–11, PCR from individual cells that were found positive for mtDNA deletions. Lanes 5–8, cells from a 101 year-old donor (9.1, 12, 3.7 and 12.5 kb, respectively); lanes 9–11, cells from the 102 year-old donor (11.5, 3.7 and 6.3 kb, respectively). M (marker lane), 1 kb ladder, lowest band, 3 kb.

Inspection of Figure 2 leads to several conclusions. First, the mitochondrial genomes with deletions are not distributed homogeneously within the tissue but are concentrated to a significant fraction in a few individual cells. Second, each of those deletion-rich cells contains only one type of deletion and different cells contain different types. We conclude that in each of these cells a single initial mutational event was succeeded by an increase in the number of mutant mtDNA copies, each of which was a descendant of the original mutant copy ('clonal expansion'). Third, each species of deleted mtDNA (with one exception) was detected only once. Assuming that we were sampling randomly from a pool of deleted mtDNA of different types and given that 13 samples out of 14 appeared to be different, we conclude that the number of different types of deletions that are present in the tissue in measurable amounts may be quite large. Interestingly, none of the deleted mtDNA species we detected is identical with the 'common' 4977 bp deletion, which was shown to be the most frequent deleted mtDNA species in certain mitochondrial diseases (19).

We have screened more than 350 individual cells from seven donors aged 31 to 109 years. As shown in Figure 3, which represents the distribution of deletion-enriched cells among donors of different ages, deletions were found in 14 cells, all of which were from centenarian samples. The finding of 14 cells with deletions in 189 centenarian cells and 0 in 165 cells from younger donors is significant at the 99% confidence level assuming a Poisson distribution.

Tests for artifacts

Given the fact that PCR is capable of generating artificial deletions, it is important to eliminate the possibility that the deletions reported above are merely PCR artifacts. The deletions we observed occurred only in a small fraction of samples, and in those samples their fraction was relatively high. This indicates that if the deletions

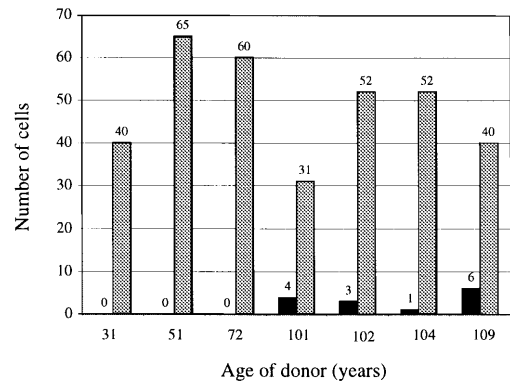


Figure 3. Distribution of cells enriched in deleted mtDNA among tissues of different ages. The histogram represents the number of cells which were not (gray) or were (black) enriched in deleted mtDNA in the heart tissue of each of seven subjects aged between 31 and 109 years.

were PCR artifacts, they would fall within a class of PCR artifacts called 'jackpots' (20). Jackpots are polymerase errors that arise in early PCR cycles, when only a small number of templates are available for replication; as a result, their apparent fraction in a given sample may be rather high. However, the probability of such an early event is low, so these errors will show up as strong bands, sporadically occurring in rare samples, i.e. exactly as we observed in our experiments. To eliminate the possibility that the observed deletions were PCR jackpots, we performed replicate PCR with DNA from each cell, which demonstrated the presence of additional bands. This was possible because only 1/10 of DNA isolated from a single cell was routinely used for a PCR. If the deletions that we observed were PCR jackpots (or low frequency random aberrant events of any other origin), they would not be observed in duplicate reactions. This is because it is very unlikely that a low frequency random event will take place in duplicate PCR from the same cell. The presence of all the deletions reported in this communication was confirmed by duplicate PCR. Several candidate deletions which failed to appear in a duplicate PCR were discarded, even though they may have represented mutation events at very low copy number.

Figure 4 shows examples of replicate PCR amplifications from a few single cell DNA samples, which were considered candidates for containing deletions based on the first PCR amplification. According to our criterion, the presence of a deletion in cells 1 and 2 (lanes 1a, 1b, and 2a, 2b, respectively) was confirmed, while in cells 3 and 4 (lanes 3a, 3b, 3c, and 4a, 4b, 4c) it was rejected. Additional confidence that the deletions we detect are not PCR artifacts is conferred by the fact that these deletions are distinct from any of the set of 'background deletions' that arise reproducibly when a deletion-free sample is subjected to many cycles of PCR (Fig. 2, lane 2). These bands represent the PCR deletional 'hotspots', i.e. the set of deletions which are generated by the thermostable polymerase at relatively high rates. If the deletions we detect in the cells were PCR artifacts, one would expect them to belong to this set of PCR hotspots.

In addition, we have determined the breakpoints of most of the deletions isolated so far (11 of 14; examples are shown in Table 1). Determination of the breakpoints, in conjunction with our use of internal nested primers for the second round of PCR, provides a final demonstration that the deleted species are of mitochondrial origin.

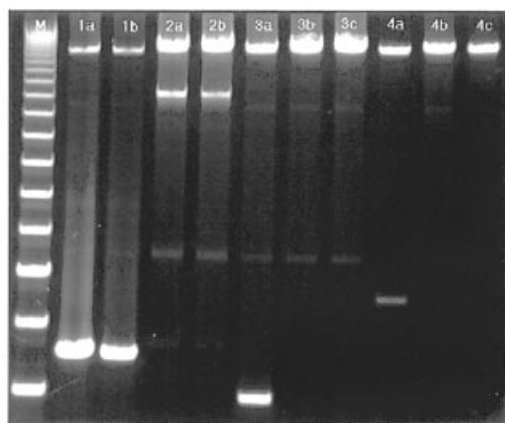


Figure 4. Test for PCR artifacts: examples of replicate PCR amplifications from DNA of individual cardiomyocytes. Each of four sets of lanes 1 (a, b), 2 (a, b), 3 (a, b, c) and 4 (a, b, c) represents a set of independent PCR amplifications of DNA from one of four single cells, respectively. Each of the four cells was initially considered a candidate carrier of a deleted mtDNA based on the presence of a short PCR fragment (lanes 1a, 2a, 3a and 4a). In two of the four cells duplicate PCR amplifications confirmed the presence of deleted mtDNA species 3.7 and 11.5 kb long (lanes 1b and 2b, respectively). In the other two cells, duplicate PCR amplifications failed to confirm the presence of deleted mtDNA although PCR were replicated twice (lanes 3b, 3c and 4b, 4c). M (marker lane), 1 kb DNA ladder, the lowest band is 3 kb.

Estimation of the fractions of deleted mtDNA in the cells

The ratio of the shorter (deleted) to the full-length (wild-type) PCR fragments in a single cell PCR does not reflect the original ratio of wild-type to deleted mtDNA in the cell. As a rule, shorter fragments amplify with a higher efficiency and become over-represented in the final PCR product. To infer the original fraction of a deletion in the cell, the ratio of the deleted to the full-length product must be corrected for the difference in amplification efficiency between the two [*'allelic preference'* (21)].

To determine the relative amplification efficiencies we performed reconstruction experiments. We prepared mixtures containing known amounts of the deleted and the full-length PCR fragments. The relative amounts of the deleted and the wild-type template in each reconstructed mixture were chosen close to the anticipated ratio in the cell. After an appropriate dilution (the dilutions were selected so as to keep the PCR within the log/linear range), these mixtures were amplified $\sim 10^2$ - and 10^4 -fold (8 and 16 cycles), and the ratios of deleted to full-length PCR fragments compared to the pre-PCR mixture were determined for each type of deleted mtDNA. The averaged results of this experiment performed in triplicate are shown in Figure 5.

As seen in Figure 5, the fraction of deleted mtDNA increases upon amplification, which reflects the fact that shorter PCR fragments are amplified with higher efficiency than the full-length product. The relative efficiencies can be calculated from the slopes of the graphs. The graphs are essentially straight lines, which enables us to extrapolate the results obtained for a 10^4 -fold amplification to the $\sim 10^9$ -fold amplification used to amplify mtDNA from individual cells. The reasoning is as follows: if 10^4 -fold amplification resulted in an x -fold increase of the ratio of deleted to full-length mtDNA, as documented by the reconstruction experiment, then a 10^9 -fold initial amplification of the

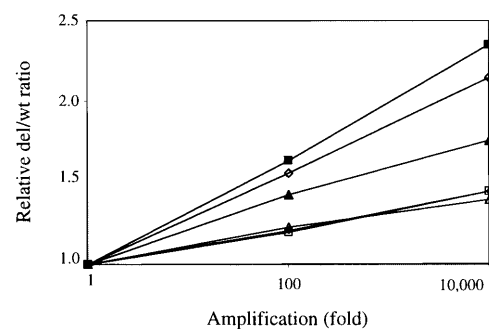


Figure 5. Relative amplification efficiency of deleted mtDNA of different sizes. Reconstructed mixtures of deleted and full-length mtDNA PCR fragments were subjected to a 100- and a 10^4 -fold amplification. The change of the ratio of deleted versus full-length species relative to the ratio in the initial mixture (average of three experiments) is plotted against the extent of amplification. Deleted mtDNA species 12.5, 12, 11.5, 9.1, 6.3 and 3.7 kb are represented by open squares, filled diamonds, open triangles, filled triangles, open diamonds and filled squares, respectively.

cellular mtDNA should have resulted in a $x^{9/4}$ -fold increase of the ratio. Consequently, to infer the original ratio in the cell, we have to divide the apparent post-PCR ratio (as determined by gel densitometry) by the $x^{9/4}$ correction factor. The estimates of the original fraction of deleted mtDNA in a few typical deletion-enriched cells are shown in Table 1 (these are the same cells which were characterized by PCR in Figure 2, lanes 5–11).

Table 1. Estimated fractions of deleted mtDNA in typical deletion-enriched cells

Size and position of breakpoints (if available) of deleted mtDNA present in the cell	Number of independent PCR amplifications from the cell	Average estimated fraction of deleted mtDNA in the cell (\pm root mean deviation)
12.5 kb	5	0.11 \pm 0.08
12 kb	2	0.22 \pm 0.12
11.5 kb: 8,036/13,095	6	0.19 \pm 0.03
9.1 kb: 6,836/14,380	5	0.24 \pm 0.08
6.3 kb: 4,069/14,306	6	0.05 \pm 0.036
3.7 kb: 3,212/16,071	3	0.64 \pm 0.3
3.7 kb: 3,212/16,071	6	0.024 \pm 0.022

The data presented in Table 1 show that estimates of the fractions of deleted mtDNA in individual cells are characterized by relatively large variances. We presume that the uncertainty of the estimates stems primarily from the sampling error associated with starting from extremely low copy numbers of deleted mtDNA. Indeed, if we typically harvest about 1000 full-length mtDNA copies per single cell, then, since only 1/10 of it is used for a PCR, each PCR starts from about 100 of total copies of mtDNA. Hence, a deleted mtDNA present at 2% fraction will on average be represented by only two copies. Obviously, the sampling error in such a situation is expected to be quite high. Consistent with this interpretation, the relative variance appears to be smaller for the cells with higher deletion fractions.

Comparison of single cells with homogenized tissue

To obtain a complementary view of the distribution of deletions in the tissue, we also performed long PCR on DNA isolated from homogenized tissue rather than individual cells. The results of such analyses of the tissues from the 31 and the 101 year-old donor are presented in Figure 2, lanes 3 and 4, respectively.

PCR products from homogenized samples do not contain any prominent bands in addition to the wild-type. Instead, they contain multiple low intensity bands. This is exactly what would be expected based on our single-cell data. Indeed, we may now consider that each low-intensity band represents one or several cells containing a high fraction of the corresponding deletion. In a mixture of large numbers of cells, such as tissue homogenate, many different deletions originating from different deletion-enriched cells would be represented, resulting in multiple bands. Given that deletion-positive cells are rare and any of many possible deletions may occur in a given positive cell, the intensity of any particular band is expected to be low, as observed.

When dealing with low intensity bands it is necessary to exclude 'background bands' discussed above, which are comparable in intensity to the bands representing real mutational events. Comparison of lanes 2 and 4 of Figure 2 shows that DNA of the 101 year-old donor contains, in addition to the 'background bands', multiple fragments corresponding to deleted mtDNA molecules. On the contrary, PCR of DNA of the 31 year-old donor (lane 3) shows mostly the 'background deletions'. These differences between the middle-aged and centenarian donors are consistent with our findings in single cells. We note, however, that quantification and analysis of images such as lane 4 of Figure 2, which contains multiple, closely spaced, low intensity bands complicated by the background, is extremely difficult and unreliable. This was one of the reasons why we decided to measure deleted mtDNA in tissues by single cell PCR, which produces, in addition to all other advantages, much simpler pictures, which are easier to analyze.

DISCUSSION

We report that scanning of the whole mitochondrial genomes of more than 350 individual cardiomyocytes from the hearts of three middle-aged and four centenarian donors revealed that most of the cells had no mtDNA deletions, while in some cells as much as one-third of mitochondrial genomes carried a deletion. Each cell carried only one type of deleted mtDNA, while different cells carried different types, as if accumulation of deleted mtDNA in the cells were a result of clonal expansion of a single initial mutational event. Interestingly, such deletion-rich cells were found exclusively in the hearts of centenarians, where they occurred at a frequency of up to about one in seven cells.

Our data are consistent with the results of others, which indicate that mtDNA deletions accumulate to high fractions in certain cells within tissue while most cells remain deletion-free (6–8). The novelty of our data is that in contrast to previous studies of single cells, which concentrated on one or a few types of deletions, we were able to detect all possible large deletions in each cell. As a result, our study does more than merely confirm previous reports that mtDNA deletions are clustered, it goes further to estimate the overall percentage of cells in tissue that are affected by any possible mtDNA deletion. The fact that as many one in seven of heart myocytes in very old people are affected by mtDNA

deletions (Fig. 3) suggests that these mutations could have a role in the aging process. On the other hand, our data rule out the possibility that deleted mtDNA represent the major mtDNA constituent of the aged heart, as suggested by some studies (22).

It is worth considering possible mechanisms that could cause clonal expansion of deleted mtDNA observed in these experiments. Traditionally, this phenomenon was explained by preferential amplification of shorter mtDNA species or preferential survival of mitochondria carrying mutated mtDNA (reviewed in 23). It is possible, however, that the 'clonal expansion' is merely a result of genetic drift of mitochondrial genotypes within individual cells. It has been shown that in the mouse, such genetic drift operates in the female germline (24) and in the colon (25). We have recently hypothesized that similar mechanisms may be also operative in post-mitotic tissues including heart, where it could be driven by constant turnover of mtDNA (26). We are currently testing this hypothesis by measuring cell-to-cell distribution of neutral mitochondrial haplotypes in the heart of a heteroplasmic mouse (25).

Are the fractions of deletions that we observe in the deletion-rich cells (2–65%; see Table 1) sufficient to cause physiological effects? First, the presence of deleted mtDNA could directly affect the activities of the mtDNA-encoded enzymes. Indeed, a reduction of mtDNA copy number in transgenic mice by ~37% results in a 40% decrease of activity of mitochondrial complex I enzymes in the heart (27). Furthermore, the observed mtDNA deletions may account for the increased susceptibility of the aged heart tissue to stress by facilitating apoptosis. Indeed, cells carrying mtDNA mutations are more vulnerable to oxidative stress-induced apoptosis, presumably due to facilitated mitochondrial permeability transition (28). It is conceivable, therefore, that when a cell containing a subpopulation of mitochondria with mutated mtDNA (such as a deletion-rich cell) is subjected to stress, the defective mitochondria would undergo a premature permeability transition, releasing cytochrome c, a known apoptosis initiator (29). In this way, even a small subpopulation of mitochondria with mutated mtDNA could predispose the whole cell to undergo apoptosis even without affecting mitochondrial function of the cell to any measurable extent. This hypothesis seems to gain support in recent experiments by Peter Zassenhaus, who constructed transgenic mice harboring mutation-prone mitochondrial DNA polymerase gamma, expressed specifically in the heart (30). mtDNA mutant fractions in the hearts of these mice are significantly increased compared to the non-transgenic control mice, approaching one mutation per mtDNA molecule, which is close to the levels anticipated in old humans (see below). Interestingly, these mice display early-onset severe dilated cardiomyopathy and significantly increased rates of (presumably apoptotic) cell death, although no defects in mitochondrial function have been detected, as would be expected if apoptoses were caused by a small subpopulation of defective mitochondria.

Our data on deletions in homogenized tissue can be compared to those published by other groups in the field. The results reported here are consistent with those reported by Reyner and Malthiery for skeletal muscle (14). These authors also observed a predominance of the full-length PCR product in both old and young donors, while the old donors presented multiple additional low intensity deletion bands absent in the young. Predominance of full-length mtDNA in old skeletal muscle was also observed by Melov and co-authors (31), who used direct Southern blotting of restriction digested (not PCR-amplified) mtDNA. However,

other groups have reported that full-length mtDNA was a minor subspecies compared to deleted mtDNA in the muscle as well as in the heart of old donors (15,22). Ozawa and co-workers reported that only 11% of mtDNA in the heart of a 97 year-old donor were full length (22). Our single cell data do not support these latter observations of extremely high fractions of mtDNA deletions in the aged heart. We therefore wondered whether our cell-by-cell analysis could have missed some cells rich in deleted mtDNA (e.g., due to their higher fragility) and thus underestimate the total load of deletions. The fact that the data on homogenized tissue (lanes 3 and 4 of Fig. 2) are consistent with our cell-by-cell analysis indicates that losses of this kind are unlikely.

The data reported in this communication may underestimate the importance of mtDNA mutations because they provide information about mtDNA deletions only. To obtain the complete picture, it would be necessary to also scan individual cells for somatic point mutations as well. Full-length mtDNA amplification from single cells described in this paper puts this seemingly enormous task within reach. Once mitochondrial genomes from a single cell are PCR amplified and are available in large quantities, it is possible to scan them for point mutations by any of a number of scanning methods. Work is in progress to scan individual cells for mtDNA point mutations using a low cost 'two-dimensional gene scanning assay' (TDGS) (32). This assay can measure virtually all possible point mutations in the most critical 25% of the mitochondrial genome, using full-length amplified mtDNA as input. However, TDGS can only be used to scan somatic mutations in single cells and cannot be applied to homogenized tissue. The reason is that TDGS (as well as other scanning approaches) is not designed to detect low frequency mutations. We and others have shown that typical frequencies of mtDNA mutations in human tissues are $<10^{-3}$ (33), which is well below the sensitivity of TDGS (~10%). However, when individual cells are concerned, the situation is different. There are indications that, similar to deletions, mtDNA point mutations accumulate in individual cells of healthy tissues (25). This means that, in individual cells of the tissue, we may expect to see relatively high fractions of point mutants, likely similar to those we observe for deletions and readily detectable by TDGS. Even more important, those mutants which are not detectable in single cells by TDGS because the mutant fraction is too low are probably not relevant to the physiology of these particular cells, and hence of the tissue as a whole.

The ability to scan the whole mitochondrial genome of individual cells for mutations is important in two respects. First, it will allow us for the first time to estimate the total load of mtDNA mutations in human tissues. Preliminary data (H.A. Collier, unpublished observation) indicate that overall load of point mutations in various organs and especially in the old heart may be well above that of deletions and could reach the level where on average, every mtDNA molecule will be hit by a mutation. If these data are confirmed, the importance of mtDNA mutations in aging will be strongly supported. Second, it gives the means to directly address the question of whether mtDNA mutations are relevant to physiology. It has been shown that aging of various organs (e.g., heart, muscle, liver) is associated with the development of a mosaic of cells differing in their bioenergetic capacity, as revealed by histological staining (15,34,35). If scanning of individual cells demonstrates that the defective but not the normal cells of the mosaic harbor appropriate fractions of mtDNA mutations, then involvement of mtDNA mutations in the

aging process is strongly supported. Work is in progress to target scanning for mtDNA mutations to cells that display decreased mitochondrial transmembrane potential upon staining with rhodamine 123 (following the staining strategy of Ames and colleagues; 35). Similarly, to test the above hypothesis that mtDNA mutations might be predisposing cells to apoptosis, one could stain the tissue for early apoptotic events (e.g., in response to an appropriate stress), isolate positive cells and then scan their mitochondrial genomes for all possible mutations.

An approach similar to that described herein has been reported in a recent paper by Linnane and co-authors (36) published while this communication was under review. Linnane and colleagues used long PCR to detect deleted mtDNA in individual skeletal muscle fibers with respect to their cytochrome c oxidase status. Although the method used by the authors is similar to that used by ourselves, their results differ from ours in several respects. First, the overall level of deletions reported in (36) is much higher than that which we and others (14,31) have observed: almost every cell tested contained at least some deletions, and a significant proportion of cells appeared to contain deletions only and no wild-type mtDNA at all. Second, most of the cells studied in (36) apparently contained multiple deletions, while in our hands each cell contained not more than one type of deleted mtDNA. One possibility is that these discrepancies reflect the differences between skeletal muscle and myocardium. We are planning to extend our measurements to skeletal muscle to test this hypothesis.

In conclusion, the presence of large fractions of mtDNA mutations in a sizable subpopulation of cardiomyocytes in the aged heart indicates that such mutations have the potential to be one of the causes of aging of the human heart. Further studies of cell-to-cell distribution of mtDNA mutations will allow us to infer their role in the aging process with a higher degree of certainty.

ACKNOWLEDGEMENTS

The authors are grateful to Dr William C. Quist (Beth Israel Deaconess Medical Center) for his suggestions on the isolation of human cardiomyocytes. We also wish to thank Dr Ravi Misra (Medical College of Wisconsin) and Dr Alla A. Kloss (University of Illinois) for critical reading of the manuscript. This work was supported in part by grants from National Institutes of Health: CA77044, AG13314, AG10829, AG00251, AG08812, AG00294, National Institutes of Environmental Health Sciences: ES02109, ES07168, ES04675, ES03926 and the Department of Energy: DE-FG02-86.

REFERENCES

- 1 Linnane, A.W., Marzuki, S., Ozawa, T. and Tanaka, M. (1989) *Lancet*, **1**, 642–645.
- 2 Bandy, B. and Davison, A.J. (1990) *Free Radical Biol. Med.*, **8**, 523–539.
- 3 Lee, C.M., Weindruch, R. and Aiken, J.M. (1997) *Free Radical Biol. Med.*, **22**, 1259–1269.
- 4 Ozawa, T. (1997) *Physiol. Rev.*, **77**, 425–464.
- 5 Hayashi, J., Ohta, S., Kikuchi, A., Takemitsu, M., Goto, Y. and Nonaka, I. (1991) *Proc. Natl Acad. Sci. USA*, **88**, 10614–10618.
- 6 Mita, S., Schmidt, B., Schon, E.A., DiMauro, S. and Bonilla, E. (1989) *Proc. Natl Acad. Sci. USA*, **86**, 9509–9513.
- 7 Shoubridge, E.A., Karpati, G. and Hastings, K.E. (1990) *Cell*, **62**, 43–49.
- 8 Collins, S., Rudduck, C., Marzuki, S., Dennett, X. and Byrne, E. (1991) *Biochim. Biophys. Acta*, **1097**, 309–317.

- 9 Moraes,C.T. and Schon,E.A. (1996) *Methods Enzymol.*, **264**, 522–540.
- 10 Schwarze,S.R., Lee,C.M., Chung,S.S., Roecker,E.B., Weindruch,R. and Aiken,J.M. (1995) *Mech. Ageing Dev.*, **83**, 91–101.
- 11 Wang,E., Wong,A. and Cortopassi,G. (1997) *Mutat Res.*, **377**, 157–166.
- 12 Muller-Höcker,J., Seibel,P., Schneiderbanger,K. and Kadenbach,B. (1993) *Virchows Archiv A*, **422**, 7–15.
- 13 Melov,S., Lithgow,G.J., Fischer,D.R., Tedesco,P.M. and Johnson,T.E. (1995) *Nucleic Acids Res.*, **23**, 1419–1425.
- 14 Reynier,P. and Malthiery,Y. (1995) *Biochem. Biophys. Res. Commun.*, **217**, 59–67.
- 15 Kovalenko,S.A., Kopsidas,G., Kelso,J.M. and Linnane,A.W. (1997) *Biochem. Biophys. Res. Commun.*, **232**, 147–152.
- 16 Katsumata,K., Hayakawa,M., Tanaka,M., Sugiyama,S. and Ozawa,T. (1994) *Biochem. Biophys. Res. Commun.*, **202**, 102–110.
- 17 Mangalam,H. (1999) <http://homet.bio.uci.edu/~hjm/projects/tacg/tacg2.main.html>
- 18 Li,H., Gyllensten,U., Cui,X., Saili,R., Erlich,H. and Arnheim,N. (1988) *Nature*, **335**, 414–417.
- 19 Moraes,C.T., DiMauro,S., Zeviani,M., Lombes,A., Shanske,S., Miranda,A.F., Nakase,H., Bonilla,E., Werneck,L.C., Servidei,S., Nonaka,I., Koga,Y., Spiro,A.J., Bronwell,A.K.W., Schmidt,B., Schotland,D.L., Zupanc,M., DeVivo,D.C., Schon,E.A. and Rowland,L.P. (1989) *N. Engl. J. Med.*, **320**, 1293–1299.
- 20 Cha,R.S. and Thilly,W.G. (1995) In Dieffenbach,C.W. and Dveksler,G.S. (eds), *PCR Primer: A Laboratory Manual*. Cold Spring Harbor Laboratory Press, Plainview, NY, pp. 37–51.
- 21 Keohavong,P. and Thilly,W.G. (1989) *Proc. Natl Acad. Sci. USA*, **86**, 9253–9257.
- 22 Hayakawa,M., Katsumata,K., Yoneda,M., Tanaka,M., Sugiyama,S. and Ozawa,T. (1996) *Biochem. Biophys. Res. Commun.*, **226**, 369–377.
- 23 de Grey,A. (1997) *Bioessays*, **19**, 161–166.
- 24 Jenuth,J.P., Peterson,A.C., Fu,K. and Shoubridge,E.A. (1996) *Nat. Genet.*, **14**, 146–151.
- 25 Jenuth,J.P., Peterson,A.C. and Shoubridge,E.A. (1997) *Nat. Genet.*, **16**, 93–95.
- 26 Marcelino,L.A. and Thilly,W.G. (1999) *Mutat. Res.*, in press.
- 27 Larsson,N.G., Wang,J., Wilhelmsson,H., Oldfors,A., Rustin,P., Lewandoski,M., Barsh,G.S. and Clayton,D.A. (1998) *Nat. Genet.*, **18**, 231–236.
- 28 Wong,A. and Cortopassi,G. (1997) *Biochem. Biophys. Res. Commun.*, **239**, 139–145.
- 29 Green,D.R. and Reed,J.C. (1998) *Science*, **281**, 1309–1311.
- 30 Zassenhaus,P. (1998) *Mitochondria: Genetics, Health and Disease*. National Institutes of Health, Bethesda, MD. <http://www-lecb.ncifcrf.gov/~zullo/mitominiDB/1998NIHMito.html>
- 31 Melov,S., Shoffner,J.M., Kaufman,A. and Wallace,D.C. (1995) *Nucleic Acids Res.*, **23**, 4122–4126.
- 32 van Orsouw,N.J., Zhang,X., Wei,J.Y., Johns,D.R. and Vijg,J. (1998) *Genomics*, **52**, 27–36.
- 33 Khrapko,K., Coller,H.A., Andre,P.C., Li,X.-C., Hanekamp,J.S. and Thilly,W.G. (1997) *Proc. Natl Acad. Sci. USA*, **94**, 13798–13803.
- 34 Muller-Höcker,J. (1989) *Am. J. Pathol.*, **134**, 1167–1173.
- 35 Hagen,T.M., Yowe,D.L., Bartholomew,J.C., Wehr,C.M., Do,K.L., Park,J.Y. and Ames,B.N. (1997) *Proc. Natl Acad. Sci. USA*, **94**, 3064–3069.
- 36 Kopsidas,G., Kovalenko,S.A., Kelso,J.M. and Linnane,A.W. (1998) *Mutat. Res.*, **421**, 27–36.